SOILS AND FOUNDATIONS Vol. 22, No. 4, Dec. 1982
Japanese Society of Soil Mechanics and Foundation Engineering

GROUNDWATER ANALYSIS OF UNDERGROUND CAVERN BY MEANS OF ROCK BLOCK MODEL

KUNIAKI SATO* and MASATO IIZAWA**

ABSTRACT

With respect to the groundwater analysis involving tunnels and caverns in rock, most papers have presented the problems on the basis of the assumption that the porous media were undeformable. Because of the dynamic deformation between fissures and rock masses due to water pressure, the groundwater motion will be affected by the deformable medium in addition to the excavation of underground structures.

This paper aims at an examination of hydraulic behavior and the analysis of groundwater flow by a rock block model which behaves as an elastic body affected by the dynamic change of fissure water pressure. A new equation, which takes the vertical distribution of permeability into consideration is proposed based on both theory and field investigations. By this equation, the groundwater movement around the cavern is analyzed by the rock block model in a confined stratum of fractured rock. Results obtained from the finite difference method are examined by some laboratory experiments, which were carried out by using a rock block model composed of a number of cubic blocks and a cavern. Comparing their numerical and experimental results, it is found that the seepage flow analysis of the underground cavern by means of the rock block model may be valid for not only the analysis of flow around the cavern but also the hydraulic modelling of seepage motion in rock masses.

Key words : analysis, fissure, groundwater, model test, rock mass, underground structure (**IGC** : G 5/E 7)

INTRODUCTION

Groundwater flow in rock masses has somewhat proper characters such as the predominant existence of dynamic deformation between fissures and rocks due to water pressure, non-isotropy of inter-connected pore space, and complicated boundary conditions. Difficulties often involve how to model a flow field and how to solve the problems under given conditions. Until now, several hydrodynamic models of flow have been proposed by some authors, in order to describe the seepage flow through rock masses. A simple model of a fractured channel is known as one-dimensional flow of viscous

* Associate Professor, Hydroscience and Geotechnology Laboratory, Faculty of Engineering, Saitama University, Urawa, Saitama.
** Electric Power Development Co., LTD, Tokyo.

Manuscript was received for review on September 2, 1981.
Written discussions on this paper should be submitted before October 1, 1983.

fluid in a parallel interstice, which can be derived from a rigorous solution of the Navier-Stokes equation. This model is not able to explain the spacial structure of a flow field and to describe the dynamic deformation of a porous medium. Some authors presented a network model consisting of a number of interstices to explain the spacial structure of fissured channels (Scheidegger, 1972). Considering the dynamic deformation of rock masses and the compressibility of water, Sato (1980) proposed a single joint model of a fractured channel. With respect to a somewhat different concept of double porosity, Barenblatt et al. (1960) gave a double porosity model of fractured rocks consisting of the primary and secondary porosities like a fractured sandstone. Warren et al. (1963) and Duguid et al. (1977) examined flow in fractured porous media by using the double porosity model. Snow (1968) proposed unique model of a rock block with due regard to the dynamic deformation of fractured rocks and the compressibility of fluid. However, until now, there is no study on hydraulic analysis of cavern and tunnel by means of such new models taking permeability change, deformation of fracture and unsteady void pressure into consideration.

In order to apply the rock block model to the groundwater flow around a cavern, at first, a new relationship concerning to the vertical distribution of permeability will be introduced by both theory and field investigations. In the next place, the groundwater movement around the cavern is analyzed by the rock block model for fractured rocks, and results obtained from the finite difference method with numerical computation are discussed by the aid of some laboratory experiments in a rock aquifer made from a number of cubic blocks having a cavern model.

PERMEABILITY DISTRIBUTIONS IN FRACTURED ROCKS

One of the most important paramenters

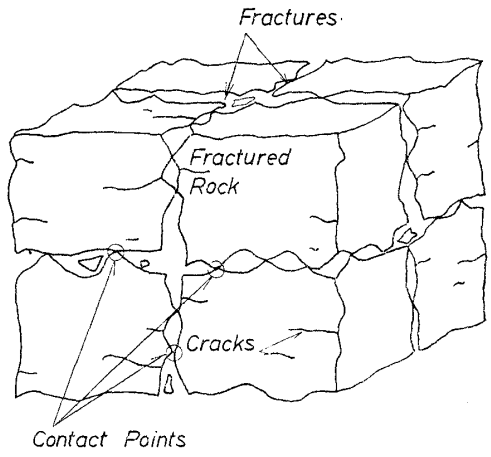

Fig. 1. Fractured rock masses

for the flow through fractured rocks is the permeability which may be distributed in a spacially inter-connected system of channels. In general, the formation and origin of inter-connected pores of fissures, which become flow channels in rock masses, may be very complicated geologically, and may be developed by various causes. The size and direction of each channel vary in geometry. However, the seepage flow will occur in micro-cracks and interstitial channels, provided the rock texture itself is much less permeable. In this study we shall pay attention to a rock ground, as demonstrated in Fig. 1. This stratum is assumed to be saturated by water, and the permeability of the micro-cracks in rock texture is negligibly small. In addition, it is assumed that the elastic deformation of contact points of irregular void walls and rock texture itself by the fluid pressure change in voids is permitted.

Then, another rock block model is introduced as shown in Fig. 2, instead of fractured rocks mentioned above. The rock block model is the same as that proposed by Snow (1968). In this model a small column in each interstice is used instead of contact points of irregular void walls, and it behaves as an elastic body subjected to a change in effective stress.

Here, the spacial distribution of permeabilities in the case of hydrostatic state is introduced by using the rock block model in

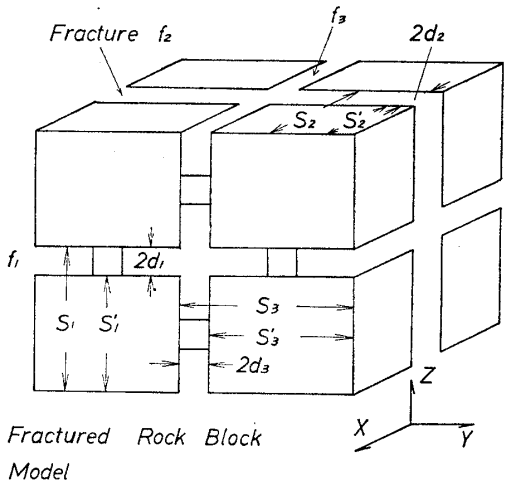

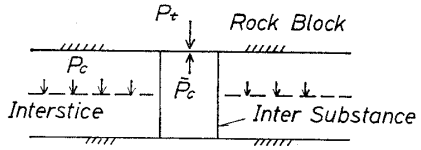

Fig. 2. Rock block model

the following theory. Referring to Fig. 2, the fluid or hydraulic conductivity k is generally given by

$$k=\frac{1}{3}\frac{g}{\nu}d^2 \qquad (1)$$

for one-dimensional flow of viscous fluid in a parallel interstice, in which g: the acceleration of gravity, ν: the kinematic viscosity of fluid, and $2d$: the width of interstice. Eq. (1) can be rewritten by introducing a concept of spacing, as Snow (1968) has proposed, for a unit block of fractured rock as

$$k_f=k\frac{2d}{s}=\frac{2}{3}\frac{g}{\nu}\frac{d^3}{s} \qquad (2)$$

where s: the spacing given by the sum of a size of block. Eq. (2) defines a permeability for a unit block like an element of rock block medium.

The total stress of void p_{ti} at an arbitrary depth of fractured rocks is assumed to be the sum of the effective stress acting on an inter-substance p_{ci} and the fluid pressure of void p_f, and this assumption is valid, after the total pressure is changed. Namely, because the contact area of inter-substance is assumed to be negligibly small, their equations are written by

$$\left.\begin{aligned} p_{ti}&=p_f+p_{ci} \\ \Delta p_{ti}&=\Delta p_f+\Delta p_{ci} \quad i=1,2,3 \end{aligned}\right\} \qquad (3)$$

in which i is the number of directional fractures. By the change of total pressure the spacing s_i and the width of interstice $2d_i$ are written by

$$\left.\begin{aligned} s_i&=s_i'+2d_i \\ \Delta s_i&=\Delta s_i'+\Delta 2d_i \end{aligned}\right\} \qquad (4)$$

$$\left.\begin{aligned} 2d_i&=2d_{0i}+\Delta 2d_i \\ s_i&=s_{0i}+\Delta s_i \end{aligned}\right\} \qquad (5)$$

in which Δ is the difference, s_i' is the size of a block, and the suffix 0 indicates the initial stage. The displacement due to a dynamic change in total stress $\Delta 2d_i$ is given by, for the inter-substance in a void,

$$\Delta 2d_i=-\frac{2d_{0i}}{a_iE_c}\Delta p_{ci}+\frac{2d_{0i}M_c}{E_c}\Delta p_f \qquad (6)$$

where E_c: the elasticity modulus of inter-substance, which is an elastic model of fracture deformation resulting from the outer forces and its material depends on the characters of the fractures. M_c: Poisson's ratio of inter-substance, and a_i: a ratio of contact areas of rock block and rectangular column ($a_i \ll 1$).

In Eq. (6), the effective stress Δp_{ci} can be eliminated by Eq. (3) as follows:

$$\left.\begin{aligned} \Delta 2d_i&=\frac{2d_{0i}}{a_iE_c}\{(1+a_iM_c)\Delta p_f-\Delta p_{ti}\} \\ &\fallingdotseq\frac{2d_{0i}}{a_iE_c}(\Delta p_f-\Delta p_{ti}) \end{aligned}\right\} \qquad (7)$$

since $a_iM_c \ll 1$.

On the other hand, the strain of rock block $\Delta s_i'/s_{0i}'$ resulting from total pressure change is given by the theory of elasticity as

$$\frac{\Delta s_i'}{s_{0i}'}=-\frac{1}{E_r}(\Delta p_{ti}-M_r\Delta p_{tj}-M_r\Delta p_{tk}) \qquad (8)$$

in which j, $k=1,2,3$, $i \neq j \neq k$, E_r: the elasticity modulus of rock block, and M_r: Poisson's ratio of rock block. In order to find the width of interstice $\Delta 2d_i$ and the spacing s_i from Eqs. (4) and (5) after the total stress is changed, the boundary condi-

tion for rock block aquifer is required. For the sake of simplicity, an infinite horizontal stratum is assumed. In this case, because the strain of rock block $\Delta s_i'/s_{0i}'$ is constant at infinite horizontal distance, Eq. (8) becomes

$$\frac{\Delta s_i}{s_{0i}}=0 \qquad (9)$$

for the case of $i=j=k\neq 1$.

The boundary condition for Eq. (9) is that the size of rock block s_i' and the width of interstice $2d_i$ are changeable by the total stress change under the constant spacing for the horizontal direction.

Then, the difference of total stress Δp_{ti} for horizontal directions of i, $j=2, 3$, $i\neq j$ is found by using Eqs. (9), (7) and (8) as

$$\Delta p_{ti}=\frac{\{(1+\lambda_j)+\lambda_i M_r\}\Delta p_f+\{\lambda_i(1+\lambda_j)M_r+\lambda_i\lambda_j M_r^2\}\Delta p_{t1}}{\{(1+\lambda_i)(1+\lambda_j)-\lambda_i\lambda_j M_r^2\}} \qquad (10)$$

$$\lambda_i=a_i\frac{E_c}{E_r}\frac{s_{0i}'}{2d_{0i}}=a_i e_c\frac{s_{0i}'}{2d_{0i}},\quad e_c=\frac{E_c}{E_r} \qquad (11)$$

Accordingly, the variation of interstice $\Delta 2d_i$ for the condition Eq. (9) is given by substituting Eq. (10) into Eq. (7) as follows:

$$\Delta 2d_i=s_{0i}'\left(\alpha_{ia}\frac{\Delta p_f}{E_r}-\alpha_{ib}\frac{\Delta p_{t1}}{E_r}\right) \qquad (12)$$

$$\left.\begin{aligned}\alpha_{ia}&=\left[\frac{(1-M_r)\{(1+M_r)\lambda_j+1\}}{(1+\lambda_i)(1+\lambda_j)-M_r^2\lambda_i\lambda_j}\right]\\ \alpha_{ib}&=\left[\frac{M_r\{(1+M_r)\lambda_j+1\}}{(1+\lambda_i)(1+\lambda_j)-M_r^2\lambda_i\lambda_j}\right]\end{aligned}\right\} \qquad (13)$$

for i, $j=2, 3$, $i\neq j$.

The strain of spacing $\Delta s_i/s_{0i}$ becomes zero from Eq. (9).

In addition, the variation of horizontal interstice $\Delta 2d_1$ is written from Eq. (7) as

$$\Delta 2d_1=\frac{2d_{01}}{a_1 e_c}\left(\frac{\Delta p_f}{E_r}-\frac{\Delta p_{t1}}{E_r}\right) \qquad (7)'$$

The strain in the vertical direction due to spacing variation is allowable, while the variation in the horizontal direction is not allowed. Then, Δs_1 is obtained by substituting Eqs. (10), (7)' and (8) into Eq. (4).

$$\Delta s_1=s_{01}'\left(\beta_{1a}\frac{\Delta p_f}{E_r}-\beta_{1b}\frac{\Delta p_{t1}}{E_r}\right) \qquad (14)$$

$$\left.\begin{aligned}\beta_{1a}&=M_r(2-\lambda_2\alpha_{2a}-\lambda_3\alpha_{3a})+\frac{1}{\lambda_1}\\ \beta_{1b}&=1-M_r(\lambda_2\alpha_{2b}+\lambda_3\alpha_{3b})+\frac{1}{\lambda_1}\end{aligned}\right\} \qquad (15)$$

As a result, the width of interstice and the spacing for each direction affected by the variations of total stress Δp_{t1} and void pressure of fluid Δp_f become from Eq. (5)

$$2d_1=2d_{01}\left\{1+\frac{1}{a_1 e_c}\left(\frac{\Delta p_f}{E_r}-\frac{\Delta p_{t1}}{E_r}\right)\right\} \qquad (16)$$

$$2d_i=2d_{0i}\left\{1+\frac{s_{0i}'}{2d_{0i}}\left(\alpha_{ia}\frac{\Delta p_f}{E_r}-\alpha_{ib}\frac{\Delta p_{t1}}{E_r}\right)\right\} \qquad (17)$$

$$s_1=s_{01}\left\{1+\frac{s_{01}'}{s_{01}}\left(\beta_{1a}\frac{\Delta p_f}{E_r}-\beta_{1b}\frac{\Delta p_{t1}}{E_r}\right)\right\} \qquad (18)$$

$$s_i=s_{0i},\quad i,j=2,3,\quad i\neq j. \qquad (19)$$

The permeability in each direction can be found by using the expression of Eq. (2) from Eqs. (16), (17), (18) and (19) as follows:

$$k_1=k_{01}\frac{\left\{1+\frac{1}{a_1 e_c}\left(\frac{\Delta p_f}{E_r}-\frac{\Delta p_{t1}}{E_r}\right)\right\}^3}{1+\frac{s_{01}'}{s_{01}}\left\{\beta_{1a}\frac{\Delta p_f}{E_r}-\beta_{1b}\frac{\Delta p_{t1}}{E_r}\right\}} \qquad (20)$$

$$k_i=k_{0i}\left\{1+\frac{s_{0i}'}{2d_{0i}}\left(\alpha_{ia}\frac{\Delta p_f}{E_r}-\alpha_{ib}\frac{\Delta p_{t1}}{E_r}\right)\right\}^3 \qquad (21)$$

$$k_{0i}=\frac{2}{3}\frac{g}{\nu}\frac{{d_{0i}}^3}{s_{0i}}\quad i=1,2,3 \qquad (22)$$

where k_{0i} is the permeability at the initial state. From Eqs. (20), (21) and (22), one can find the permeability in each direction for the variations of void pressure Δp_f and total stress Δp_{t1}, if the contact area and elasticity modulus E_c of inter-substance, the size of rock block s_{0i}', the elasticity modulus of rock block E_r, the Poisson's ratio of rock block M_r, and the width of interstice at the initial state d_{0i} are given for required flow. It is noted that the variation of void pressure Δp_f is produced by falling of piezometric head in case of groundwater motion around the cavern, if the total stress in rock ground is constant. It can be found in Eq. (20) that permeability of a horizontal fracture, k_1 is approximately governed by the parameter $a_1 e_c$, because the denominator

in Eq. (20) becomes nearly 1. In addition, the second term of Eq. (21) is very small for an ordinary rock.

GOVERNING EQUATION OF FLOW

In an ordinary way, the governing equation of groundwater movement can be introduced by the equation of motion and the continuity equation. In many cases, Darcy's law can be applied as the equation of motion, since the inertia of flow is negligibly small in rock masses having the fissures and fractures of small opening not more than several hundred microns. For the flow through fractured rock masses, the deformation of rocks and the change of fluid density by pore pressure become very important. Here, the governing equation on the basis of the rock block model will be derived from the quantities described in early paragraph of this study as the same manner as Snow's model.

As is well known, the continuity relation of a control volume $\Delta x \Delta y \Delta z$ is

$$-\left\{\frac{\partial}{\partial x}(\rho q_x)+\frac{\partial}{\partial y}(\rho q_y)+\frac{\partial}{\partial z}(\rho q_z)\right\}\Delta x\Delta y\Delta z = \left\{n_0\frac{\partial \rho}{\partial t}\Delta z+\rho\frac{\partial n_0}{\partial t}\Delta z+\rho n_0\frac{\partial(\Delta z)}{\partial t}\right\}\Delta x\Delta y \tag{23}$$

in which x, y, and z: the co-ordinates, ρ: the density of fluid, q_x, q_y and q_z: the velocity in x, y and z directions, respectively, n_0: the porosity, and t: the time.
The righthand terms of Eq. (23) must be rewritten for the rock block model. The first term is written by

$$\frac{\partial \rho}{\partial t}=\rho\frac{\gamma_w}{E_w}\frac{\partial h_f}{\partial t} \tag{24}$$

where γ_w: the unit weight of fluid, E_w: the compressibility of fluid, and $h_f=p_f/\rho g$.
The porosity n_{0i} of each interstice is defined as

$$n_0=n_{01}+n_{02}+n_{03},\quad n_{0i}=\frac{2d_i}{s_i}\quad i=1,2,3. \tag{25}$$

From Eqs. (16), (17), (18) and (19), the porosity in each interstice is given by

$$n_{01}=\frac{2d_{01}}{s_{01}}\frac{\left\{1+\frac{1}{a_1e_c}\left(\frac{\Delta p_f}{E_r}-\frac{\Delta p_{t1}}{E_r}\right)\right\}}{\left\{1+\frac{s_{01}'}{2s_{01}}\left(\beta_{1a}\frac{\Delta p_f}{E_r}-\beta_{1b}\frac{\Delta p_{t1}}{E_r}\right)\right\}} \tag{26}$$

$$n_{0i}=\frac{2d_{0i}}{s_{0i}}\left\{1+\frac{s_{0i}'}{2d_{0i}}\left(\alpha_{ia}\frac{\Delta p_f}{E_r}-\alpha_{ib}\frac{\Delta p_{t1}}{E_r}\right)\right\} \tag{27}$$

for i, $j=2,3$, $i\neq j$.
Generally speaking, the time rate of porosity change n_{0i} is written by

$$\frac{\partial n_{0i}}{\partial t}=\frac{\partial n_{0i}}{\partial p_f}\frac{\partial p_f}{\partial t}+\frac{\partial n_{0i}}{\partial p_{t1}}\frac{\partial p_{t1}}{\partial t}$$

Thus, the term $\partial n_{0i}/\partial t$ can be expressed by

$$\frac{\partial n_{01}}{\partial t}=\eta_a\frac{\gamma_w}{E_r}\frac{\partial h_f}{\partial t}-\eta_b\frac{\gamma_w}{E_r}\frac{\partial h_t}{\partial t} \tag{28}$$

$$\frac{\partial n_{0i}}{\partial t}=\frac{s_{0i}'}{s_{0i}}\alpha_{ia}\frac{\gamma_w}{E_r}\frac{\partial h_f}{\partial t}-\frac{s_{0i}'}{s_{0i}}\alpha_{ib}\frac{\gamma_w}{E_r}\frac{\partial h_t}{\partial t} \tag{29}$$

in which

$$\eta_a=\frac{\frac{s_{01}}{s_{01}'}-a_1e_c\beta_{1a}+(\beta_{1a}-\beta_{1b})\frac{\gamma_w}{E_r}\Delta h_{t1}}{\lambda_1\left\{\frac{s_{01}}{s_{01}'}+\beta_{1a}\frac{\gamma_w}{E_r}\Delta h_f-\beta_{1b}\frac{\gamma_w}{E_r}\Delta h_{t1}\right\}^2}$$

$$\eta_b=\frac{\frac{s_{01}}{s_{01}'}-a_1e_c\beta_{1b}+(\beta_{1a}-\beta_{1b})\frac{\gamma_w}{E_r}\Delta h_f}{\lambda_1\left\{\frac{s_{01}}{s_{01}'}+\beta_{1a}\frac{\gamma_w}{E_r}\Delta h_f-\beta_{1b}\frac{\gamma_w}{E_r}\Delta h_{t1}\right\}^2}$$

where $h_{t1}=p_{t1}/\rho g$ (written by h_t in above equations for the sake of simplicity).
Accordingly, the term $\partial n_0/\partial t$ is obtained as

$$\frac{\partial n_0}{\partial t}=\left(\eta_a+\frac{s_{02}'}{s_{02}}\alpha_{2a}+\frac{s_{03}'}{s_{03}}\alpha_{2a}\right)\frac{\gamma_w}{E_r}\frac{\partial h_f}{\partial t}-\left(\eta_b+\frac{s_{02}'}{s_{02}}\alpha_{2b}+\frac{s_{03}'}{s_{03}}\alpha_{3b}\right)\frac{\gamma_w}{E_r}\frac{\partial h_t}{\partial t} \tag{30}$$

The third term of Eq. (23) is expressed by

$$\frac{\partial(\Delta z)}{\partial t}=\frac{\Delta z}{s_1}\frac{\partial s_1}{\partial t}=\frac{\Delta z}{s_{01}+\Delta s_1}\frac{\partial(\Delta s_1)}{\partial t}=\frac{\Delta z/s_{01}}{1+\Delta s_1/s_{01}}\frac{\partial(\Delta s_1)}{\partial t},\quad \Delta s_1/s_{01}\ll 1=\frac{\Delta z}{s_{01}}\frac{\partial(\Delta s_1)}{\partial t}$$

since $d(\Delta z)/\Delta z=d(s_1)/s_1$ is assumed.
Then, the third term is written from Eq. (14) as

$$\frac{\partial(\Delta z)}{\partial t}=\left(\frac{s_{01}'}{s_{01}}\beta_{1a}\frac{\gamma_w}{E_r}\frac{\partial h_f}{\partial t}-\frac{s_{01}'}{s_{01}}\beta_{1b}\frac{\gamma_w}{E_r}\frac{\partial h_t}{\partial t}\right)\Delta z \tag{31}$$

As a result, by putting $\partial h_f/\partial t=\partial h/\partial t$, $h=h_f+z$: the piezometric head, and using Darcy equations

$$q_x=-k_x\frac{\partial h}{\partial x},\quad q_y=-k_y\frac{\partial h}{\partial y},\quad q_z=-k_z\frac{\partial h}{\partial z} \tag{32}$$

Eq. (23) becomes from Eqs. (24), (30) and (31) as follows:

$$\frac{\partial}{\partial x}\left(k_x\frac{\partial h}{\partial x}\right)+\frac{\partial}{\partial y}\left(k_y\frac{\partial h}{\partial y}\right)+\frac{\partial}{\partial z}\left(k_z\frac{\partial h}{\partial z}\right)=S_f\frac{\partial h}{\partial t}-S_t\frac{\partial h_t}{\partial t} \tag{33}$$

in which,

$$S_f=\left(\frac{n_0}{e_w}+\eta_a+\frac{s_{02}'}{s_{02}}\alpha_{2a}+\frac{s_{03}'}{s_{03}}\alpha_{3a}+n_0\frac{s_{01}'}{s_{01}}\beta_{1a}\right)\frac{\gamma_w}{E_r}$$

$$S_t=\left(\eta_b+\frac{s_{02}'}{s_{02}}\alpha_{2b}+\frac{s_{03}'}{s_{03}}\alpha_{3b}+n_0\frac{s_{01}'}{s_{01}}\beta_{1b}\right)\frac{\gamma_w}{E_r}$$

and $e_w=E_w/E_r$.

In Eq. (33), $S=S_f+S_t$ on the righthand side may be considered as a storage coefficient per unit thickness of aquifer. Specific storage S_s ($10^{-4}\sim10^{-7}$/m) in the governing equation for ordinary aquifer like sand includes all dynamic factors such as deformation of soil particles, voids and fluid, and permeability change. It must be noted that Eq. (33) explains clearly such dynamic factors for the flow through rock masses. Eq. (33) is the governing equation of flow through the rock block medium.

Referring to Fig. 2, the permeabilities k_x, k_y and k_z for the x, y and z directions are defined by

$$\left.\begin{aligned}k_x&=k_1+k_3\\k_y&=k_1+k_2\\k_z&=k_2+k_3\end{aligned}\right\} \tag{34}$$

CAVERN MODEL AND NUMERICAL COMPUTATION SCHEMES

In order to examine the groundwater behavior around the cavern, a simple flow field model is introduced as shown in Fig. 3. In this model the cavern is rectangular, and

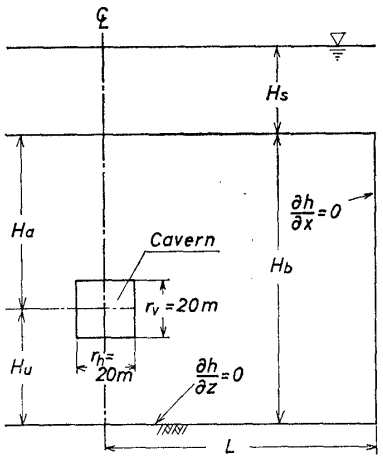

Fig. 3. Cavern model in confined groundwater

the fractured rock ground is covered with a weathered layer. There are several types of caverns in practice; for example, the electric power station, the oil storage cavern. Here, an oil storage cavern having a recharge water tunnel is demonstrated in Fig. 12, as one of examples. The flow can be regarded as the confined one in horizontal rock masses. In this study, unsteady behavior of groundwater will be examined for those types of flow in the following paragraphs.

Numerical computation schemes by the finite difference method are presented in the following manner. Governing equation of the flow becomes as

$$\frac{\partial}{\partial x}\left(k_x\frac{\partial h}{\partial x}\right)+\frac{\partial}{\partial z}\left(k_z\frac{\partial h}{\partial z}\right)=S_f\frac{\partial h}{\partial t} \tag{35}$$

for vertically two-dimensional flow by ignoring the unsteady effect originated from the total stress variation in Eq. (33). In addition, boundary conditions are adopted by

$$\left.\frac{\partial h}{\partial x}\right]_{x=L}=0 \tag{36}$$

$$\left.\frac{\partial h}{\partial z}\right]_{\text{at impervious bottom}}=0 \tag{37}$$

$$h_c]_{\text{at wall of cavern}}=z+p_g/\rho g:\ \text{const.} \tag{38}$$

$h=h_0$: at upper boundary of fractured rocks (39)

$h=h_r$: at wall of recharge tunnel (40)

in which p_g: the pressure in cavern, h_0: the piezometric head at upper boundary of fractured rock ground, and h_r: the head in

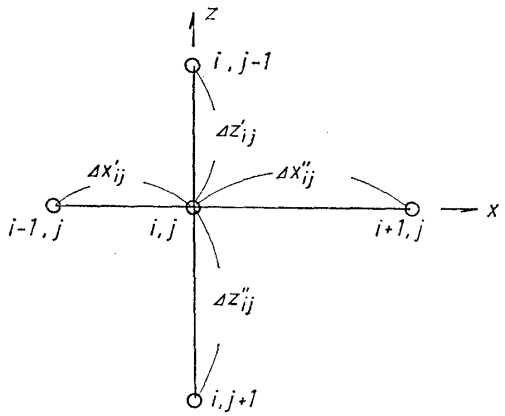

(a) **Finite difference scheme of arbitrary mesh intervals**

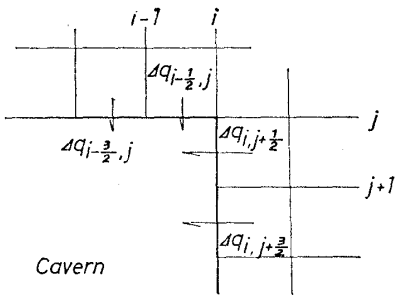

(b) **Computation scheme of flow rate**

Fig. 4. Computation schemes

recharge tunnel.

With respect to the finite difference scheme of Eq. (35) Crank-Nikolson method is adopted by Tanaka and Aki (1979), since the difference meshes are not the same in flow field. Eq. (35) is written from Fig. 4 (a) as

$$S_{fij}{}^{n}\frac{h_{ij}{}^{n+1}+h_{ij}{}^{n}}{\Delta t}=\frac{1}{2}\{f^{n+1}(h)+f^{n}(h)\}+\frac{1}{2}\{g^{n+1}(h)+g^{n}(h)\} \tag{41}$$

in which,

$$f(h)=\frac{\Delta x' k_{xi+1/2,j}h_{i+1,j}-(\Delta x' k_{xi+1/2,j}+\Delta x'' k_{xi-1/2,j})h_{ij}+\Delta x'' k_{xi-1/2,j}h_{i-1,j}}{\frac{\Delta x'\Delta x''(\Delta x'+\Delta x'')}{2}}$$

$$g(h)=\frac{\Delta z' k_{zi,j+1/2}h_{i,j+1}-(\Delta z' k_{zi,j+1/2}+\Delta z'' k_{zi,j-1/2,j})h_{ij}+\Delta z'' k_{zi,j-1/2}h_{i,j-1}}{\frac{\Delta z'\Delta z''(\Delta z'+\Delta z'')}{2}}$$

$$k_{xi+1/2,j}=\frac{2k_{xi+1,j}k_{xij}}{k_{xi+1,j}+k_{ij}}$$

$$k_{xi-1/2,j}=\frac{2k_{xi-1,j}k_{xij}}{k_{xi-1,j}+k_{xij}}$$

$$k_{zi,j+1/2}=\frac{2k_{zi,j+1}k_{zij}}{k_{zi,j+1}+k_{zij}}$$

$$k_{zi,j-1/2}=\frac{2k_{zi,j-1}k_{zij}}{k_{zi,j-1}+k_{zij}}$$

Then, practical computation is carried out by means of the Over-Relaxation Method by Tanaka and Aki until the convergence value $\varepsilon=10^{-4}$ is satisfied by repeating m times

$${}^{m+1}h_{ij}{}^{n+1}={}^{m}h_{ij}{}^{n+1}+\kappa(\tilde{h}_{ij}{}^{n+1}-{}^{m}h_{ij}{}^{n+1}) \tag{42}$$

$$\begin{aligned}\tilde{h}_{ij}{}^{n+1}=&\frac{1}{1+C_x(\Delta x' k_{xi+1/2,j}+\Delta x'' k_{xi-1/2,j})+C_z(\Delta z' k_{zi,j+1/2}+\Delta z'' k_{zi,j-1/2})}\\&\times\Big[C_x(\Delta x' k_{xi+1/2,j}{}^{m}h_{i+1,j}{}^{n+1}+\Delta x'' k_{xi-1/2,j}\cdot{}^{m+1}h_{i-1,j}{}^{n+1})\\&+C_z(\Delta z' k_{zi,j+1/2}{}^{m}h_{i,j+1}{}^{n+1}+\Delta z'' k_{zi,j-1/2}\cdot{}^{m+1}h_{i,j-1}{}^{n+1})\\&+\frac{\Delta t}{S_{fij}}\{f(h)^{n}+g(h)^{n}\}+h_{ij}{}^{n}\Big]\end{aligned} \tag{43}$$

$$C_x=\frac{\Delta t}{S_{fij}\Delta x'\Delta x''(\Delta x'+\Delta x'')}$$

$$C_z=\frac{\Delta t}{S_{fij}\Delta z'\Delta z''(\Delta z'+\Delta z'')}$$

and

$$|(\tilde{h}_{ij}{}^{n+1}-{}^{m}h_{ij}{}^{n+1})/{}^{m+1}h_{ij}{}^{n+1}|\ll\varepsilon \tag{44}$$

in which i, j: the mesh numbers and n: the time step.

Flow rate into the cavern q_c is found by

$$q_c=-k_n\frac{\partial h}{\partial n}\ :\text{at wall of cavern} \tag{45}$$

in which k_n: the permeability normal to wall, and n: the normal direction to wall, positive outward.

Referring to Fig. 4 (b), the finite difference scheme of flow rate can be given by

$$\left.\begin{aligned}\Delta q_{i-1/2,j}&=k_z\frac{h_{i-1,j-1}+h_{i,j-1}-h_{i-1,j}-h_{ij}}{2\Delta z}\Delta x\\\Delta q_{i,j+1/2}&=k_x\frac{h_{i+1,j}+h_{i+1,j+1}-h_{ij}-h_{i,j+1}}{2\Delta x}\Delta z\end{aligned}\right\} \tag{46}$$

At the impervious bottom of fractured rock ground the following scheme is satisfied:

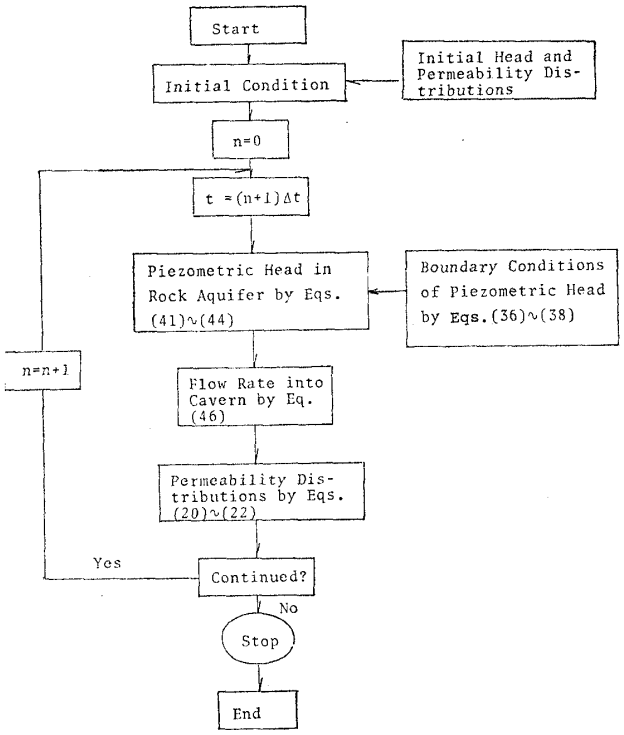

Fig. 5. Computational flow of groundwater analysis

$$\frac{h_{i,j-1}-h_{i,j+1}}{2\Delta z}=0 \qquad (37)'$$

In addition, the other boundary conditions are assumed to be constant. Computational procedure is shown in Fig. 5. Piezometric heads are computed at each finite mesh under the boundary conditions, the flow rate into the cavern is obtained, and the permeability distributions are determined from the fluid pressure and the total stress at the arbitrary time. There is no convergence problem by this finite difference method.

For all numerical computations of flow analysis around the cavern, three different mesh sizes are used for improving the accuracy: $\Delta x_1=0.2\,L/i_1$, $i_1=16$, $\Delta x_2=0.3\,L/i_2$, $i_2=12$, and $\Delta x_3=0.5\,L/i_3$, $i_3=10$ in Figs. 3, 12 and 16. The meshes become larger with distance from the cavern in a half aquifer. Physical quantities used in the computations are given by Table 1, in which the specific weight of water is $\gamma_w=1$, that of rock $\gamma_r=2.5$, that of weathered layer $\gamma_1=2.0$, the elasticity modulus of rock is $E_r=2.1\times 10^5\,\mathrm{kgf/cm^2}$ and Poisson's ratio is $M_r=0.3$ for the granite. Other conditions are given for each computation in accordance with the symbols in Figs. 3 and 12.

DISCUSSIONS OF PERMEABILITY DISTRIBUTION AND CHARACTERS OF GROUNDWATER MOTION AROUND CAVERN

Discussions of Permeability Distribution

Prior to the examination of groundwater motion around the cavern by means of the rock block model, it is very interesting to

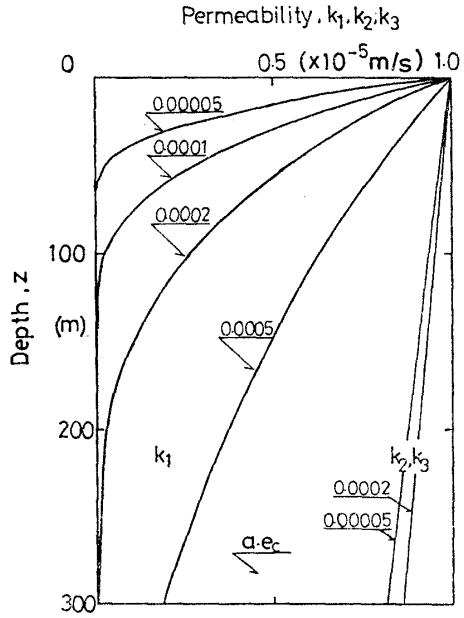

Fig. 6. Permeability distributions with depth z for different parameter ae_c

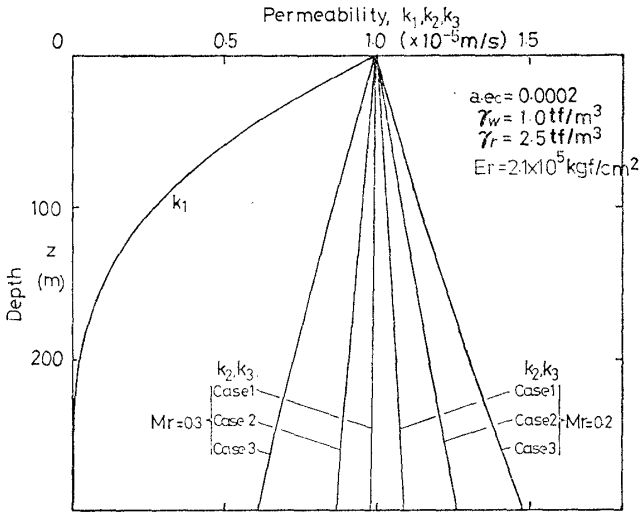

Fig. 7. Permeability distributions with depth z for different parameter M_r

Table 1. Physical quantities of numerical conditions (see Figs. 3 and 12 for notations)

Case	Block size S_0 (m)	Interstitial width $d_0\times10^{-5}$ (m)	Porosity $n_0\times10^{-4}$	Storage Ceof. $S_{f0}\times10^{-7}$m	Permeability k_0 (m/s)	Other quantities
C-S-1	0.1	5.85	35.00	34.70	10^{-5}	$ae_c=0.0002$ $\gamma_w=1.0$ tf/m^3 $L=400$ m $\gamma_r=2.5$ tf/m^3 $E_r=2.1\times10^5$ kgf/cm^2 $M_r=0.3$ $H_s=100$ m, $H_b=200$ m, $r_h=r_v=20$ m
C-S-2	1.0	12.50	1.63	9.79		
C-S-3	10.0	27.10	1.63	3.00		
C-L-1	1.0	1.51	0.603	9.79	1.72×10^{-8}	$H_0=20$ m, $H_b=122.0$ m, $H_s=10$ m, $H_a=52.0$ m $H_u=70.0$ m, $H=27.0$ m, $l=52.0$ m $r_h=15.0$ m, $r_v=18.0$ m, $\Delta H=5$ m, $\gamma_1=2.0$ tf/m^3
C-L-2						

discuss the adaptability of permeability equations proposed in early paragraphs as compared with field data. Particularly, a quantitative evaluation of the vertical and horizontal permeabilities and the comparison of parameters becomes important.

At first, two theoretical relationships between the permeabilities k_1, k_i and the depth z are given in Figs. 6 and 7 from Eqs. (20), (21) and (22) for the quantities of Table 1. In Table 1, the spacing s_{0i}, the width of interstice d_{0i}, the porosity n_{0i} and the permeablitity k_{0i} are assumed to be homogeneous and isotropic for each case at the initial condition: namely, $s_0=s_{01}=s_{02}=s_{03}$, $2d_0=2_{01}=2d_{02}=2d_{03}$, and $k_0=k_{01}=k_{02}=k_{03}$ at the initial stage $p_{f0}=0$ and $p_{t1}=0$. In order to examine basic characters of permeability change with depth and behavior of flow around cavern, all values in Table 1 were assumed on the basis of practical judgment. Fig. 6 shows the relationships between k_1, k_2, k_3 and z for ae_c as the parameter after the fluid pressure $p_f=\gamma_w z$ and the total stress $p_{t1}=\gamma_r z$ (γ_w, γ_r: the unit volume weight of fluid and rock block, respectively) are loaded in an instant. At the initial condition the permeability k_0 is the same for all cases, since d_0 and n_0 are appropriately presumed. It can be noted from Fig. 6 that the horizontal permeability k_1 will not be related with Poisson's ratio and the spacing, because the value of denominator in Eq. (20) approaches to 1, and k_1 will approach proper constant value with depth. In addition, the vertical permeability k_2 and k_3 will increase with depth if Poisson's ratio becomes small. For the distributions of k_2 and k_3 with depth z, the following interpretation is taken notice generally. From Eq. (21), k_i can be written by

$$k_i=k_{01}(1+D_a\cdot D_b)^3$$

in which D_a and D_b are given from Eqs. (11) and (13) by putting $\lambda=\lambda_2=\lambda_3$ as follows:

$$D_a=\frac{\lambda_i\alpha_{ia}}{a\cdot e_c}=\frac{(1-M_r^2)\lambda^2+(1-M_r)\lambda}{(1-M_r^2)\lambda^2+2\lambda+1}\frac{1}{a\cdot e_c}$$

$$D_b=\left(\frac{\Delta p_f}{E_r}-\frac{M_r}{1-M_r}\frac{\Delta p_{t1}}{E_r}\right),\quad \lambda=\frac{ae_c s_0'}{d_0}$$

This quantity D_a governs k_i if D_b is constant. For that case, k_i becomes larger as λ increases so $dD_a/d\lambda>0$. Namely, the spacing s_0 will be related with the distribution of k_{0i} under constant ae_c. Fig. 7 shows the permeability distributions for M_r as the parameter in case of $ae_c=0.0002$. The distribution of k_1 with depth depends largely on ae_c: namely, the strength and the size of both inter-substance and rock block become a governing factor of permeability distribution. Iwai (1976) has reported that the ratio of contact areas a is dependent on the acting stress: $a=0.001$ for the effective stress $p_c=2.6$ kgf/cm^2 and $a=0.1\sim0.2$ for $p_c=200$ kgf/cm^2 in the case of granite. At the same time, the geometrical form and weathering are closely related with e_c of the inter-substance.

On the other hand, the practical values of parameter ae_c can be determined by referring to some results of field measurements. Figs. 8 and 9 show the permeability distributions with depth by Carlson et al. (1977) in Sweden

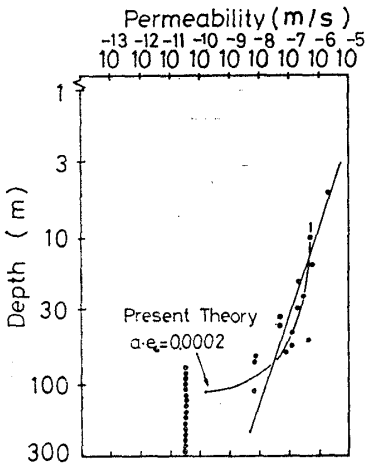

Fig. 8 (a). Comparison between permeabilities by field measurement and those by present theory (Carlson et al., 1977)

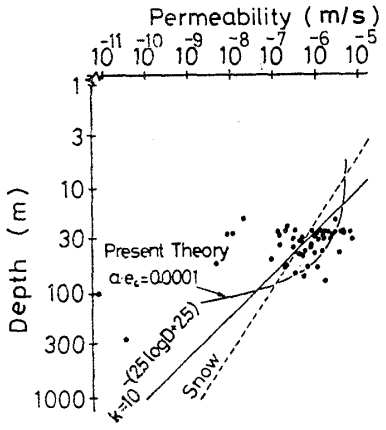

Fig. 8 (b). Comparison between permeabilities by field measurement and those by present theory (Carlson et al., 1977)

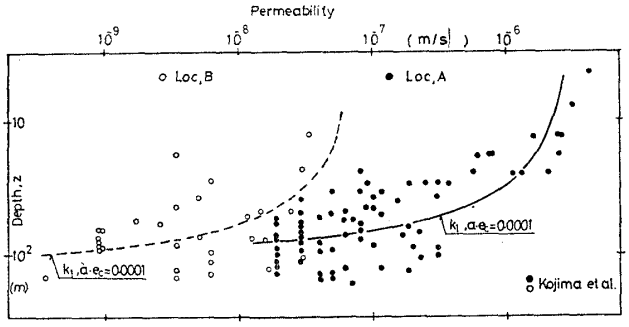

Fig. 9. Comparison between permeabilities by field measurement and ones by present theory (Kozima et al., 1980)

and Kozima et al. (1980) in Japan. Both investigations have been carried out by Lugion Test Method at the zone of granite. Permeability k_{01} at initial stage in Eq. (20) was assumed as $k_{01}=6.0\times10^{-7}$ m/s for Fig. 8 (a), 5.0×10^{-6} m/s for Fig. 8 (b), and $k_{01}=6.2\times10^{-8}$ m/s for Loc. B, 3.0×10^{-6} m/s for Loc. A in Fig. 9. In those figures the most fitted curves by Eq. (20) are shown for $ae_c=0.0001$ and 0.0002 in Fig. 8, and $ae_c=0.0001$ in Fig. 9, by letting the denominator of Eq. (20) is equal to 1. The permeability distributions with depth by field investigations are explained by the present theory, while the total stress and fluid pressure are assumed to be proportional to the depth.

Numerical Analysis of Groundwater Flow Around Cavern

Numerical analysis of groundwater flow around the cavern is carried out for three somewhat different cases: the first case is the analysis of piezometric head, the permeability and the flow rate around the cavern in a submerged confining aquifer, the second is that of a confined aquifer below a weathered layer and the third is that of the second case having a recharge tunnel above the cavern. Referring to the cavern models in Fig. 3, the computations are done according to the conditions shown in Table 1.

At the initial condition of fractured rocks, the permeability distributions are obtained by Eqs. (20), (21) and (22) as shown in Fig. 10 (a) for each case. As described before, the vertical change of permeabilities k_x and k_z is more notable as the block size becomes large. In this figure, k_{x0} and k_{z0} are the permeabilities at the surface of rock ground. Permeability distributions will change with time, if the pressure in the cavern is kept atmospheric after excavating the cavern. Results of permeability distribution computed from Eqs. (41) to (46) and (20) to (22) are given by Figs. 10 (a), (b), (c) and (d) for the conditions in Table 1. Figs. 10 (a) and (c) show the non-dimensional permeabilities k_x/k_{x0} and k_z/k_{z0} at t=2 min and $t=30$ min in a half plane, so the flow field is symmetric. Because the effective stress increases as the fluid pressure drops under constant total

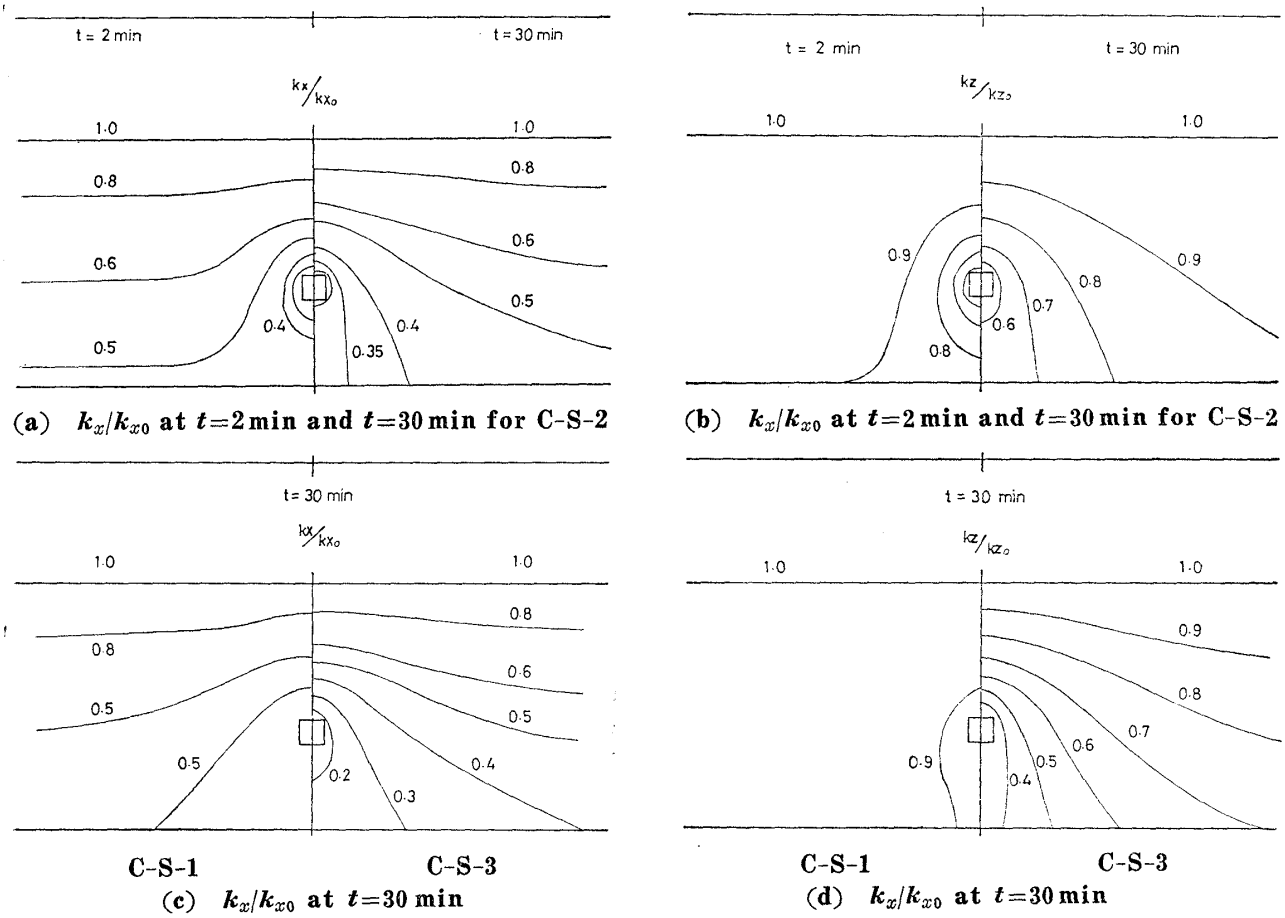

(a) k_x/k_{x0} at t=2 min and t=30 min for C-S-2

(b) k_x/k_{x0} at t=2 min and t=30 min for C-S-2

(c) k_x/k_{x0} at t=30 min

(d) k_x/k_{x0} at t=30 min

Fig. 10. Permeability distributions (in which o indicates value at surface of rock ground)

stress, the width of fractures decreases with time toward the outer zone of cavern. Namely, it is reduced to the drop of permeability in the whole aquifer. Particularly, the tendency is distinguished for horizontal permeability k_x/k_{x0}, and the change of k_x/k_{x0} with time is attained steady and stable state in early stage. Moreover, Figs. 10 (b) and (d) show the permeability distributions of k_z/k_{z0} and they mean that the change of permeability is related with the block size. Thus, final change of permeability becomes large as the block size increases. Then, the change of flow rate into the cavern is computed as shown in Fig. 11 for each case. In this figure C-S-2′ means the flow rate for which the permeabilities k_{x0} and k_{z0} are assumed constant in a whole ground for the case C-S-2. In addition, C-S-2″ is for the case of C-S-2 in which the change of effective stress with time is ignored. It may be laid down as a general rule that the degression curves of flow rate are slower than those of C-S-2′ and C-S-2″ because of the change of permeability.

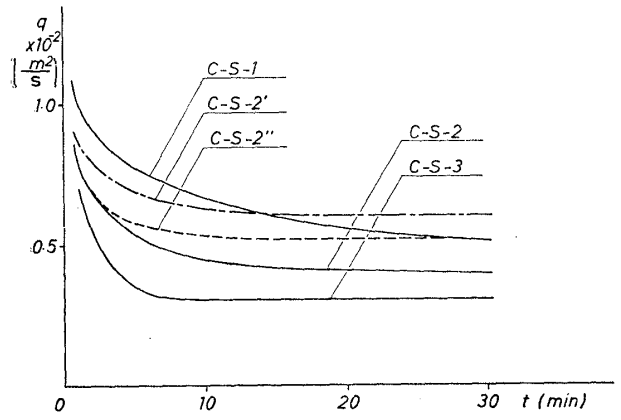

Fig. 11. Flow rate q with t (C-S-2″; constant uniform permeability of C-S-2 and C-S-2′; no change of effective stress with time for C-S-2)

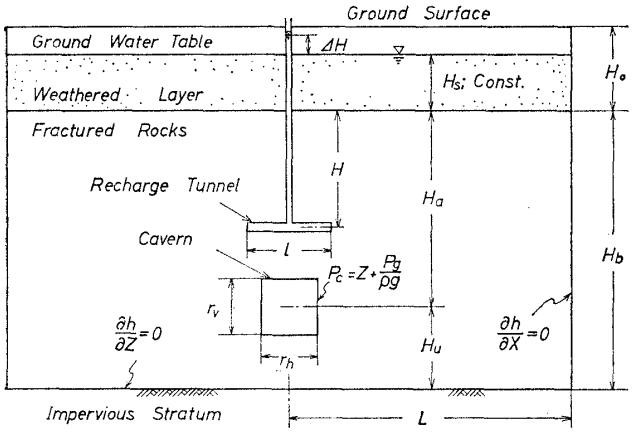

Fig. 12. Cavern model having recharge tunnel in confined ground below weathered layer

Final constant flow rate is related with the block size, and the degression velocity is abrupt in early stage for case C-S-3, since the permeability change with time is finished in a short time. By numerical analyses mentioned above, one can point out the following characteristics of the rock block

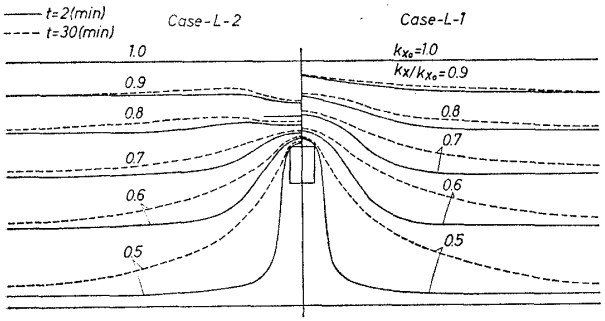

(a) k_x/k_{x0} at t=2 min and t=30 min for C-L-1 and C-L-2

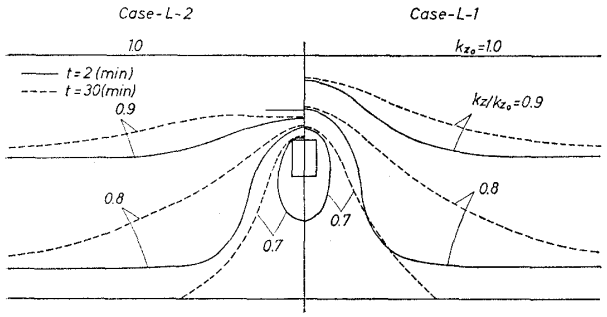

(b) k_x/k_{x0} at t=2 min and t=30 min for C-L-1 and C-L-2

Fig. 13. Permeability distributions (in which "o" indicates value at surface of rock ground)

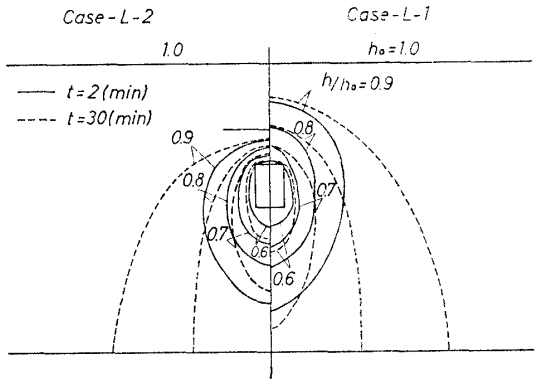

Fig. 14. Distributions of piezometric head h/h_0 at t=2 min and t=30 min for C-L-1 and C-L-2 (in which h_0 is value of h at surface of rock ground)

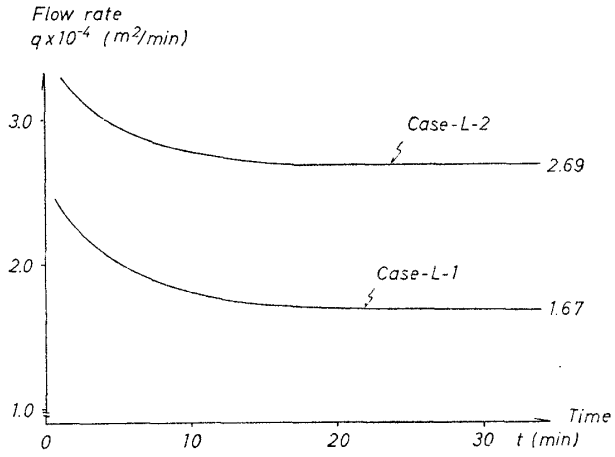

Fig. 15. Flow rate q with time t

model: the permeability change spreads over the outer zone of cavern with time, the flow rate decreases gradually and it becomes constant at final stage of time, and both permeability and flow rate depend mainly on the block spacing.

On the other hand, the permeability distribution, the piezometric head and the flow rate degression are examined for the cases in which the cavern is excavated in a confined aquifer below a weathered layer. Two cases are considered: one is the flow around a cavern of r_v=18.5 m in width and r_h=15.0 m in height, and another is that of a cavern having a recharge tunnel. The recharge tunnel is often used for the caverns for storing oil and liquefied gas to prevent the stored liquid from leaking and to conserve of groundwater. The conditions and para-

meters in the following computations are summarized in Table 1. Permeability distributions, the piezometric head distributions and the flow rate curves are computed as shown in Figs. (13) (a) and (b), Fig. 14 and Fig. 15, respectively. For each distribution in Figs. 13 and 14, the changes of distribution with time are presented for the case in which there is the recharge tunnel in the left side as compared with the case without them. In those figures the subscript "o" indicates the value at the top of fractured rock ground. Both permeability and piezometric head distributions are not so different in the neighborhood of the cavern wall, in spite of whether the recharge tunnel exists or not. However, both differences are distinct far from the cavern, so the pressure drop is limited by the recharge water supply. The flow rate into cavern increases by the existence of recharge tunnel. Because of the flow is within confined ground, unsteady state of motion becomes steady in a short time. Its character of flow is one of the most marked properties for confined groundwater movement.

Several interesting results are derived from numerical computations by the rock block model. In particular, it may be worth notice that the interstitial width of fractures decreases by the pressure drop around the cavern and the degression curve of flow rate is retarded with time. The opinion cannot be applied immediately to the ground outside the cavern wall, since the rock ground is loosened during excavation. The loosening has been observed by field measurements of Seikan tunnel to the extent of a few meters for a tunnel in tuff rock (JSCE, 1979), and not a few meters for the cavern in granite.

EXPERIMENTS AND THEIR RESULTS

Experimental Apparatus and Conditions

In order to examine the present theories and numerical analyses the experiments are carried out under appropriate conditions. Experimental apparatus is made from transparent resin, and it is 1.0 m long, 0.5 m high, and 0.06 m wide, as shown in Fig. 16. Rock ground model with a cavern is set up by using a number of transparent block as shown in Fig. 16. Four pieces of elastic gum are inserted into each horizontal interstice so as to deform in vertical direction only. Two vertical interstices are kept from deforming by small guide blocks and hard steel rods. The cavern model is located on the right of the ground model, because the flow field around the cavern is established in a left half domain of the cavern. The size of cavern is equal to only one block. Flow rate at steady state is measured by a graduated cylinder, and the ground subsidence at surface is measured by displacement gage. The fluid used in this experiment is a viscous oil having a viscosity of 4.881×10^{-4} m^2/s, and the specific weight of 0.85. The specific weight of the block model is 1.20, and the value of aE_c is 0.002 kgf/cm^2, which was determined beforehand by loading experiment of a block having elastic gum inter-substances in the viscous

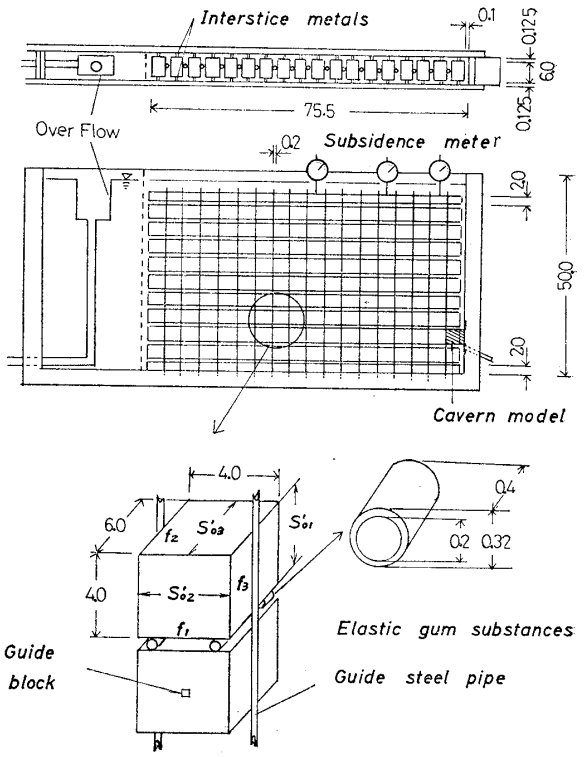

Fig. 16. Experimental apparatus (dimension : $\times 10^{-2}$ m)

Table 2. Physical quantities of experiments (see Fig. 16 for notations)

Quantities \ Fracture number	Fracture f_1	Fracture f_2	Fracture f_3
Spacing s_0 (m)	0.0432	0.0425	0.0625
Block size s_0' (m)	0.04	0.04	0.06
Fracture width $2d_0$ (m)	0.0032	0.002	0.0025
k_0 (m/s)	0.00129	0.00032	0.00022
k_{x0} (m/s)	0.00151	—	—
k_{z0} (m/s)	—	—	0.00054

oil. In this experiment the spacing s_0, the block size s_0' and the permeability k_0 at the initial condition are summarized in Table 2. All experiments were accomplished in an air conditioned room at a constant temperature (19°C~20°C) and humidity. Two cases of experiments were carried out: Run-1 is on confined flow around the model cavern for the case in which the permeability is changeable by the fluid pressure drop, and Run-2 is with constant permeability by using four pieces of small metal instead of elastic gum inter-substances. The results of both experiments will be compared and discussed below.

Experimental Procedure and Discussion of Test Results

At first, the blocks are packed in 18 columns and 10 layers by using the guide rods and elastic gum substances for Run-1 as shown in Fig. 16. For the packing of blocks the displacement in depth direction is restrained by two interstice metals, and the uppermost and lowest layers are packed by a half size block; 0.02 m in height. Viscous oil is filled in the block model after adjusting the overflow tank in the left side to keep a constant confined head H_s=0.03 m. Then, the cavern model is pulled out suddenly, and the subsidence gage is observed by photograph. In addition, final constant flow rate is measured by graduated cylinder. In that occasion, the oil pressure around the cavern model becomes atmospheric in an instant, because the cavern model is only one of the blocks. Experimental procedure of Run-2 is the same with Run-1, but four

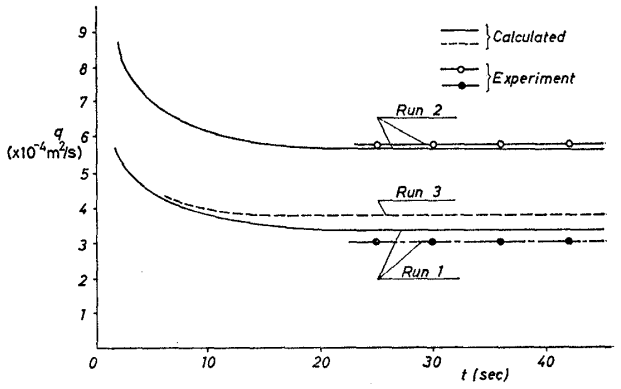

Fig. 17. Comparison between flow rate by numerical computation and one by experiment (In this figure, Run-3 is with no change of effective stress)

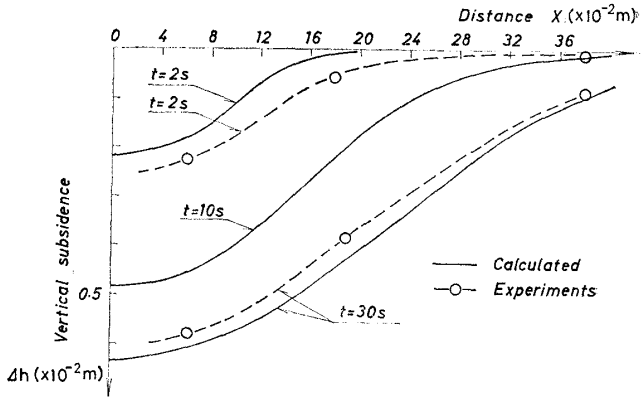

Fig. 18. Vertical subsidence

pieces of small metal are used instead of the elastic gum substances. Flow through network interstices is laminar, since Reynolds number R_e at the maximum velocity around cavern is smaller than R_e=0.26.

Comparison between numerical computation by the block model and the experimental result are shown in Fig. 17 for flow rate, and in Fig. 18 for surface subsidence. In Fig. 17, Run-3 means a computed result assuming that the initial distribution of permeability is kept constant despite the fluid pressure drops.

In spite of difficult experiments, the discrepancy between numerical solutions and experiments is small in both results of flow rate. One of the reasons why some discrepancy is induced for subsidence experiments will be the friction between the blocks and the guide rods. However, it can be concluded by the experiments that the change of flow

rate with time is well explained by the theory of rock block model, and the subsidence is induced from the change of spacing within a limit of unavoidable experimental error.

CONCLUSIONS

Hydraulic behavior in fractured rocks were studied by introducing the rock block model which behaves as an elastic porous medium subjected dynamic pore pressure. The present theory was applied to the analysis of groundwater around the cavern in fractured rock masses, and the results were examined by an experimental apparatus similar to the rock block model. Conclusions by this study are summarized as in the following.

The permeabilities in three directions can be given formally by Eqs. (20), (21) and (22). From proper character of those equations, the permeability k_1 of horizontal interstice is very changeable because the spacing s_{0i} is fixed along two vertical sides. Permeability k_1 is mainly dependent on the ratio of contact areas a_1, that of elastic moduli e_c, the change of total stress Δp_{t1} and fluid pressure Δp_f. For other directions the permeabilities k_2 and k_3 are not so large as k_1, and they are related with $a_1 e_c$, Poisson's ratio and the spacing s_{0i}.

With respect to permeability k_1 of granite, the governing parameter $a_1 e_c$ becomes 0.0001 $\sim$0.0002 for several results of field measurements.

Governing equation for the rock block model is given by Eq. (33), in which two terms S_f and S_t are interpreted as the storage coefficient in a broad sense. By using Eqs. (20), (21), (22) and (33), the flow rate change with time decreases gradually for the cavern of confined rock ground, compared with the case that the dynamic change of permeabilities are ignored. In addition, the permeability distributions in the ground change with time, and their values decrease gradually with elapsed time around the cavern since the fall in fluid pressure propagates to the outer pore channels one after another. Furthermore, the present theory was examined by means of a newly-designed apparatus for the flow model of a cavern. Validity of the theory was demonstrated within unavoidable error of difficult experiment. This joint study was carried out at Saitama University during the period when the junior author M. Iizawa was a graduate student.

REFERENCES

1) Barenblatt, G. I., Zheltov, Iu. P. and Kochina, I. N. (1960): "Basic concepts in theory of seepage of homogeneous liquids in fissured rocks," PMM, Vol. 5, No. 5, pp. 852-864.
2) Carlson, A. and Olsson, T. (1977): "Variation of hydraulic conductivity in some Swedish rock types," Rock Store, Proc. First Int. Sym. Stockholm Sweden, No. 2.
3) Duguid, J. O. and Lee, P. C. Y(1977): "Flow in fractured porous media," Water Resources Res. June, pp. 588-566.
4) Iwai, K. (1976): "Fundamental studies of fluid flow through a single fracture," Ph. D. Thesis, Univ., California, Barkeley.
5) Japan Soc. Civil Engrs. (1979): Rept. Earth Pressure Investigations of Seikan-Tunnel, pp. 61-97.
6) Kozima, K. and Watanabe, K. (1980): "Field measurements and their evaluations of geological quantities pertaining to groundwater flow in fractured rocks," Proc. Sym. Soc. Applied Geology.
7) Scheidegger, A. E. (1960): The Physics of Flow Through Porous Media, Univ. Toronto Press.
8) Snow, D. T. (1968): "Fracture deformation and changes of permeability and storage upon changes of fluid pressure," Quarterly of Colorado School of Mines, Vol. 63, NO. 1, Janu, pp. 201-244.
9) Sato, K. and Iizawa, M. (1981): "Governing equations of flow through rock masses and their characters," Proc. 25th Japanese Conference on Hydraulics, JSCE, Feb., pp. 273-378.
10) Tanaka, S. and Aki, S. (1979): "Studies on technical developments for unlined underground storage of fuel," Rept. Central Inst. Elec. Power Industry, No. 379006.
11) Warren, J. E. and Root, P. J. (1963): "The behavior of naturally fractured reservoirs," J. Soc. Petroleum Engrs. Sept, pp. 245-255.